Behavior of a single element in a finite stochastic array

José Gómez-Ordóñez, José M. Casado, and Manuel Morillo*

Área de Física Teórica, Facultad de Física, Universidad de Sevilla, Apartado de Correos 1065, Sevilla 41080, Spain

(Received 8 February 2012; revised manuscript received 30 April 2012; published 16 May 2012)

We describe statistical properties of a single element in a nonlinear stochastic array with a finite number of elements with mean-field-like (global) coupling. Desai and Zwanzig [J. Stat. Phys. **19**, 1 (1978)] made use of a self-consistent dynamic mean-field ansatz to derive, in the infinite-size limit, a nonlinear Fokker-Planck equation (NLFPE) for the single-particle distribution function. In this work we explore the reliability of this approximation to describe a finite system with a small number of elements. We carry out a numerical analysis of the NLFPE as well as numerical simulations of the full set of Langevin equations governing the dynamics of the coupled elements. We find that for parameter values such that the NLFPE has a single stationary solution, it provides a reliable asymptotic approximation to the time evolution and stationary properties of a finite system of even modest size. In contrast, for parameter values such that the NLFPE has two stable stationary coexisting solutions, the NLFPE leads to results that are greatly at variance with those obtained from the numerical simulations of the Langevin equations for small systems.

DOI: 10.1103/PhysRevE.85.051121 PACS number(s): 05.40.−a, 05.45.Xt

I. INTRODUCTION

This work deals with the statistical mechanical description of the behavior of a single element of a stochastic array with N-coupled identical elements. We will use a model that was introduced by Kometani and Shimizu [1] as a model for muscle contractions and, in its infinite-size limit, was extensively studied several years ago in a pioneering paper by Desai and Zwanzig [2]. The model describes N degrees of freedom globally coupled to each other via a mean-field-like interaction term. Each degree of freedom has an intrinsic nonlinear dynamics. The nonlinearity and the action of noise terms render the behavior of the system far from trivial. When the parameter characterizing the mean-field interaction is positive, Desai and Zwanzig were able to derive in the limit $N \to \infty$ a nonlinear Fokker-Planck equation (NLFPE) for the single-particle reduced distribution function. Their analysis of the stationary distribution showed that in the asymptotic limit, the model possesses a phase transition with a bifurcation of the probability distribution containing non-Gaussian characteristics. Later on, the critical dynamics and the fluctuations at the critical point of the model were studied also in the infinite-size limit by Dawson [3]. Shiino [4] proved an extension to the NLFPE of the usual H theorem for linear Fokker-Planck equations.

Similar models with globally coupled elements have been used to study diverse problems in diverse areas. The cooperativity of the model arising from the coupling between the individual elements and the nonlinearity and stochasticity of the dynamics give rise to an ample variety of behaviors. It is not surprising that the model itself (or similar ones) has been used to investigate the formation of public opinion [5], stochastic resonance effects in a single element [6] or in collective variables [7], noise-induced synchronization in a collective variable [8], etc. When considering systems driven by an external time periodic force, the term system-size stochastic resonance in models of coupled elements [9,10] has been used to analyze nonmonotonic behaviors of the system response with a finite number of elements in the system. Finite-size effects have also been studied recently in models of opinion formation [11], where the fact that apparent phase transitions in finite models of social behavior disappear in the thermodynamic limit has been analyzed.

In a previous work [12] we considered the statistical mechanical description of a collective variable characterizing a finite system. In the present work we focus our interest on the description of an individual degree of freedom. In Ref. [2] Desai and Zwanzig introduced an ansatz to generate what they called the self-consistent dynamics mean-field (SCDMF) approximation to describe the single-particle distribution function. This assumption leads, in the limit of an infinite system, to a NLFPE. In this work we test the reliability of this asymptotic NLFPE to describe the behavior of a single particle in an array with a finite number of elements. We proceed by numerically solving the NLFPE using the procedure described in Ref. [13]. The results obtained are compared with those provided by the numerical simulations of the whole set of Langevin equations describing the dynamics of the finite system for several values of the system size.

The structure of this paper is as follows. In Sec. II we present the Langevin and Fokker-Planck description of the N-particle model. The SCDMF approximation leading to the NLFPE proposed by Desai and Zwanzig in Ref. [2] is also briefly discussed. In Sec. III we analyze the behavior of the first two cumulant moments using numerical simulations of the full set of Langevin equations and the numerical solution of the NLFPE. The stationary single-particle distributions estimated from the simulation results are also compared with those obtained from the NLFPE. Finally, in Sec. IV we present a summary.

II. MODEL

The model can be viewed as a set of nonlinear oscillators. Each oscillator is described by a coordinate x_i so that the dynamics of the system is given by the set of coupled Langevin

*morillo@us.es

equations (in dimensionless form)

$$\dot{x}_i = x_i - x_i^3 + \frac{\theta}{N}\sum_{j=1}^{N}(x_j - x_i) + \xi_i(t), \tag{1}$$

where θ is the strength of the mean-field coupling term. This parameter will be taken to be either positive or negative. The set $\xi_i(t)$, $i = 1,2,\ldots,N$, represents N uncorrelated Gaussian white noises with zero averages and $\langle \xi_i(t_1)\xi_j(t_2)\rangle = 2D\delta_{ij}\delta(t_1 - t_2)$.

An alternative formulation of the dynamics is in terms of the linear Fokker-Planck equation for the joint probability density $f_N(x_1,x_2,\ldots,x_N,t)$,

$$\frac{\partial f_N}{\partial t} = \sum_i \frac{\partial}{\partial x_i}\left(\frac{\partial U}{\partial x_i} f_N\right) + D\sum_i \frac{\partial^2 f_N}{\partial x_i^2}, \tag{2}$$

where U is the potential energy relief

$$U = \sum_{i=1}^{N} V(x_i) + \frac{\theta}{4N}\sum_{i=1}^{N}\sum_{j=1}^{N}(x_j - x_i)^2, \tag{3}$$

with the single-particle potential

$$V(x_i) = \frac{x_i^4}{4} - \frac{x_i^2}{2}. \tag{4}$$

The term $V(x_i)$ describes a symmetrical potential with two wells of equal depths separated by a hump at $x_i = 0$. The interaction part of the full potential modifies it in such a way that for $\theta > 1$ the two wells blend into a single minimum at $x_i = 0$. For $\theta < 1$ the two wells exist, but their locations and the barrier height depend on θ. Note that for $\theta > 0$ the interaction energy contribution to the full potential favors that any pair x_i and x_j should have the same sign (both either positive or negative), while for $\theta < 0$ the opposite happens and the interaction tends to favor configurations with positive and negative values of the variable. In the long-time limit the linear Fokker-Planck equation has a unique solution given by

$$f_N^{\mathrm{st}}(x_1,x_2,\ldots,x_N) = \frac{1}{Z}\exp\left(-\frac{U}{D}\right), \tag{5}$$

where Z is a normalization function.

To study the dynamical properties of the system, Desai and Zwanzig introduced the SCDMF approximation. From Eq. (2) an infinite hierarchy of equations for the reduced probabilities $f_s(x_1,\ldots,x_s,t)$ defined as

$$f_s(x_1,\ldots,x_s,t) = \int dx_{s+1}\cdots dx_N\, f_N(x_1,x_2,\ldots,x_N,t) \tag{6}$$

can be obtained. This hierarchy is analogous to the well known Bogoliubov-Born-Green-Kirkwood-Yvon hierarchy derived from the Liouville equation for Hamiltonian systems [14]. For all practical purposes this infinite hierarchy has to be truncated at some level. In particular, the molecular chaos approximation leads to a closed equation for the single-particle distribution function. Along this line of thought, Desai and Zwanzig proposed the ansatz $f_2(x_1,x_2,t) \approx \rho_1(x_1,t)\rho_1(x_2,t)$ leading, in the $N \to \infty$ limit, to the nonlinear Fokker-Planck equation

$$\frac{\partial \rho_1}{\partial t} + \frac{\partial}{\partial x}\{[\theta X(t) - (\theta - 1)x - x^3]\rho_1\} = D\frac{\partial^2 \rho_1}{\partial x^2}, \tag{7}$$

where x represents any of the x_i variables and $X(t)$ is given by the self-consistency condition

$$X(t) = \int_{-\infty}^{\infty} dx\, x\rho_1(x,t). \tag{8}$$

Here $X(t)$ is an intensive quantity playing the role of a time-dependent order parameter for the model. We have denoted the single-particle reduced distribution function in the infinite-size limit by ρ_1. Note that the SCDMF approximation amounts to neglecting the correlation function between any two pairs of degrees of freedom. Due to the nonlinearity of Eq. (7), the possibility of coexistence of several stable single-particle probability distributions cannot be ruled out. The coexistence of several ρ_1 for the same set of parameter values is a qualitative aspect that is not present in the linear Fokker-Planck description of the N-particle dynamics.

The NLFPE has a stationary solution given by

$$\rho^{\mathrm{st}} = \frac{1}{Q}\exp\left[-\frac{1}{D}\left(\frac{x^4}{4} + (\theta - 1)\frac{x^2}{2} - \theta X_0 x\right)\right], \tag{9}$$

where Q is a normalization constant and X_0 is given by self-consistent relation

$$X_0 = \int_{-\infty}^{\infty} dx\, x\rho^{\mathrm{st}}(x). \tag{10}$$

Except for the stationary case, no other analytical solutions of the NLFPE (7) with the condition (8) are known.

Desai and Zwanzig considered the case of $\theta > 0$. Their analysis of the stationary solution shows that for some regions of the parameter space, there is just one stable probability solution of Eqs. (9) and (10) centered around a zero-order parameter $X_0 = 0$. For other regions, the system shows the coexistence of two stable probability distributions centered around nonzero values. In this way, the model within the SCDMF approximation seems to show a true phase transition and not merely a change in the shape of the stationary single distribution function from monomodal to bimodal. In Ref. [2] the boundary line separating the ordered (nonzero-order parameter) from the disordered (zero-ordered parameter) phases is depicted in the model parameter space. In addition, within the region of coexistence of two stable solutions, the system will reach one or the other depending upon the initial condition. In contrast, for $\theta < 0$ and any noise strength, the only stationary solution of Eqs. (9) and (10) corresponds to $X_0 = 0$, independently of the initial preparation.

III. NUMERICAL ANALYSIS

Analytical solutions of the multidimensional Fokker-Planck equation (2) are not known, except in the stationary long-time limit. The N-particle equilibrium distribution has a canonical form with the potential as in Eq. (3) and the noise strength D playing the role of a temperature. No closed equation for the single-particle distribution $f_1(x,t)$ for N finite exists. Even an explicit form for the stationary distribution $f_1^{\mathrm{st}}(x)$ cannot be obtained analytically from the N-particle equilibrium distribution except in the absence of coupling ($\theta = 0$). Thus, to obtain information about the behavior of a single element of a finite system we have turned to numerical simulations of the stochastic equations in Eq. (1). Using the

numerical procedure detailed in Refs. [15], we have integrated the Langevin equations for a large number of noise realizations (typically 5000 realizations). Averaging over them, we have evaluated the first two cumulant moments of a single variable given by

$$M_1(t) = \langle x(t) \rangle \approx \frac{1}{\mathcal{N}} \sum_{\alpha=1}^{\mathcal{N}} x^{(\alpha)}(t) \tag{11}$$

and

$$M_2(t) = \langle x^2(t) \rangle - M_1^2(t) \approx \frac{1}{\mathcal{N}} \sum_{\alpha=1}^{\mathcal{N}} (x^{(\alpha)})^2(t) - M_1^2(t), \tag{12}$$

where $\mathcal{N}$ indicates the total number of trajectories and $x^{(\alpha)}(t)$ indicates the numerically obtained single-particle trajectory in the α noise realization. Also binning the results for a single variable, we have constructed histograms giving estimates of the stationary solution $f_1^{\rm st}(x)$.

As noted above, analytical solutions of the NLFPE are not available except for the stationary case. Several years ago we developed a numerical scheme to solve the NLFPE (7) with the consistency condition (8) [13]. Using this numerical scheme, the single probability distribution $\rho_1(x,t)$ is propagated in time starting from a given initial condition until it reaches its stationary form $\rho^{\rm st}$ given by Eq. (9). Also, using the numerically evaluated $\rho_1(x,t)$, the time evolution of the first two cumulant moments is easily obtained by numerical quadrature $M_1(t) = X(t)$ and $M_2(t) = \int dx\, x^2 \rho_1(x,t) - X(t)^2$.

A. The case of θ positive

Let us first consider $\theta > 0$. In this case, Desai and Zwanzig distinguish four regions of parameter space separated by a boundary line (see Ref. [2]). For two of those regions, the NLFPE has more than one stable stationary distribution for a given set of parameter values, while for the other two regions, there is just one stable stationary solution, with a monomodal shape for $\theta > 1$ and bimodal for $\theta < 1$.

In Fig. 1 we depict the results obtained from the long-time limit of the NLFPEs (9) and (10) for $\theta = 2$ and $D = 1.33$. We also depict the one-particle stationary distribution function obtained using numerical simulations of the Langevin equation (1) for $N = 10, 100, 1000, 10\,000$ for the same noise and coupling strengths. It can be seen that even for systems with a small number of particles ($N = 10$), the NLFPE yields a relatively good approximation to the simulation results. For $N = 100$ and beyond, there is a very good matching of the stationary solution of the NLFPE and that provided by the simulations.

The time evolution of the first two moments $M_1(t)$ and $M_2(t)$ as obtained from the Langevin numerical simulations and from the NLFPE are depicted in Fig. 2 for the same parameter values as in Fig. 1. For the Langevin simulations, all the particles are initially at $x_i = 0.3$. For the NLFPE we take $\rho_1(x,0)$ to be a sharply peaked Gaussian centered at $x = 0.3$. We have also explored several other initial conditions. In all cases the system relaxes to its stationary situation after a transient time. Even for small N values, the NLFPE provides a very acceptable approximation of the dynamical evolution of the moments.

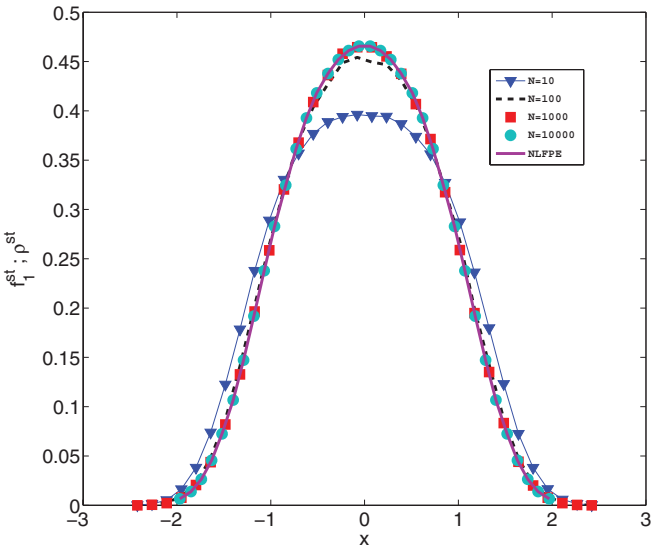

FIG. 1. (Color online) The single-particle stationary distribution function obtained from the simulations of Eq. (1) for $N = 10$ (blue triangles), $N = 100$ (black dashed line), $N = 1000$ (red squares), and $N = 10\,000$ (cyan circles) are compared with the stationary solution of the NLFPEs (9) and (10) (magenta solid line). The other parameters are $D = 1.33$ and $\theta = 2$.

Let us know consider a case where the stable stationary distribution is bimodal. In Fig. 3 we depict the results for $f_1^{\rm st}(x)$ as estimated from the simulations of Langevin equations and $\rho^{\rm st}(x)$ as the stationary solution of the NLFPE. Several system sizes have been used as indicated in the figure. Other

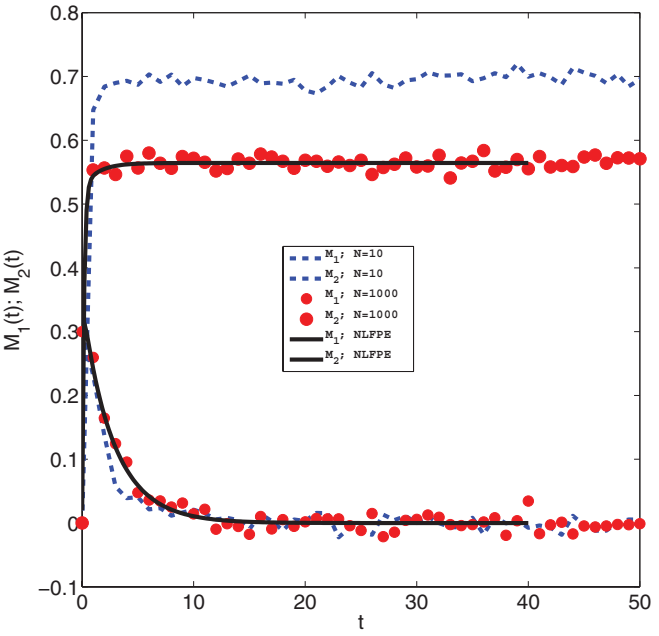

FIG. 2. (Color online) Time evolution of the first two cumulant moments $M_1(t)$ (bottom curves) and $M_2(t)$ (top curves) for $N = 10$ (blue dashed lines) and $N = 1000$ (red circles) obtained from the numerical simulations of the Langevin equations for the N degrees of freedom and from the numerical solution of the NLFPE (black solid lines). The other parameters are $D = 1.33$ and $\theta = 2$.

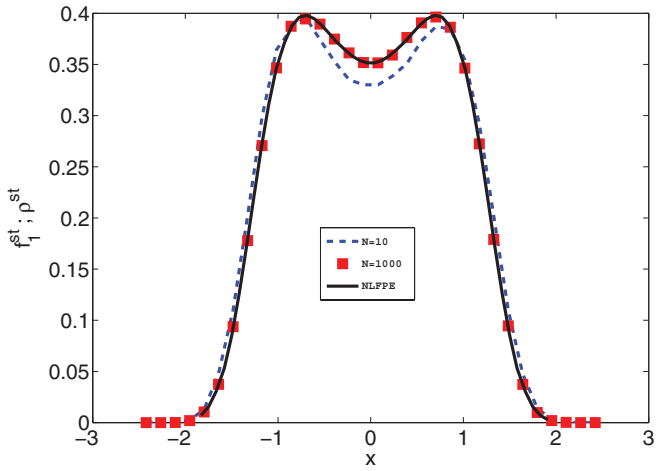

FIG. 3. (Color online) The single-particle stationary distribution function obtained from the simulations of Eq. (1) for $N = 10$ (blue dashed line) and $N = 1000$ (red squares) are compared with the stationary solution of Eq. (9) (black solid line). The other parameters are $D = 0.5$ and $\theta = 0.5$.

parameter values are $D = 0.5$ and $\theta = 0.5$. The time evolution of the first two moments is plotted in Fig. 4. Again, even for rather small systems, the NLFPE reproduces the numerical simulation results quite faithfully.

Our results indicate that the NLFPE approximation to the single-particle distribution function is an acceptable one as long as the noise strength D and the coupling parameter θ are such that the NLFPE has a single stationary solution, regardless of whether this is monomodal or bimodal.

Let us now turn our attention to those regions of parameter space where the NLFPE has two stable coexisting solutions. In

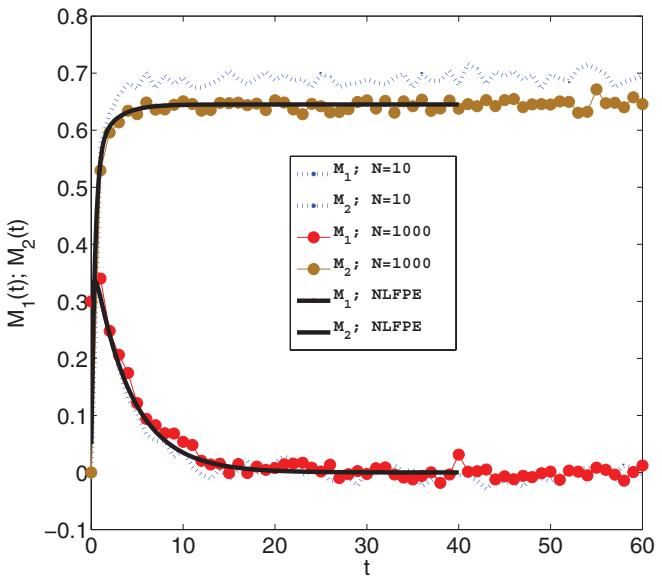

FIG. 4. (Color online) Time evolution of the first two cumulant moments $M_1(t)$ (bottom curves) and $M_2(t)$ (top curves) for $N = 10$ (blue dotted lines) and $N = 1000$ (red circles) obtained from the numerical simulations of the Langevin equations for the N degrees of freedom and from the numerical solution of the NLFPE (black solid lines). The other parameters are $D = 0.5$ and $\theta = 0.5$.

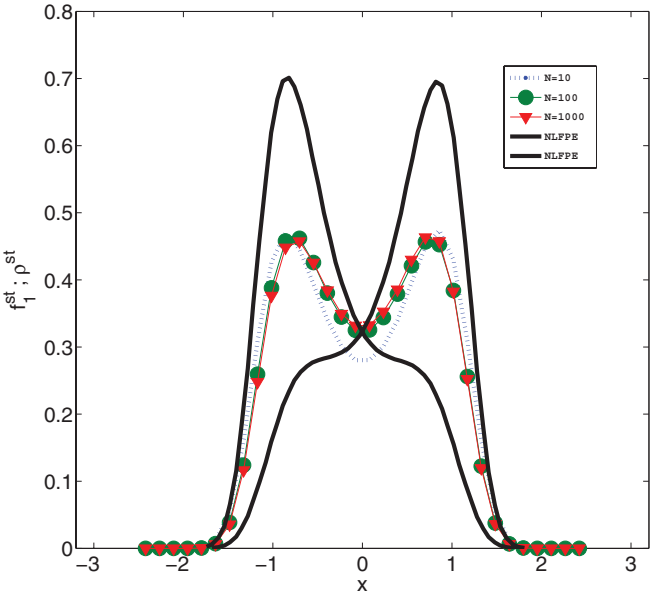

FIG. 5. (Color online) Single-particle stationary distribution function obtained from the simulations of Eq. (1) for $N = 10$ (blue dashed line), $N = 100$ (green circles), and $N = 1000$ (red triangles) is compared with the stationary solutions of the NLFPE (9) (black solid lines). The other parameters are $D = 0.25$ and $\theta = 0.5$.

Figs. 5 and 6 we present results for the probability distribution and the time evolution of the first moment. The most remarkable feature of those figures is that the NLFPE provides a picture of the finite-system dynamics that is qualitatively wrong. In Fig. 5 we note that for all finite-N systems, there is just one stationary solution with two symmetrically located maxima around a minimum at $x = 0$. Except for the height

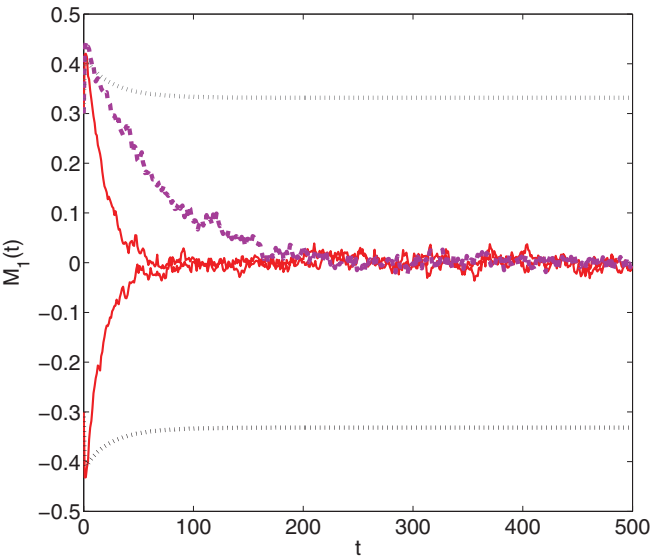

FIG. 6. (Color online) Time evolution of $M_1(t)$ obtained from the numerical simulations of the Langevin equations for $N = 10$ (red solid lines) and within the NLFPE (blue dotted lines) with two different initial conditions. The (magenta) dashed line depicts the evolution for $N = 100$ from $M(0) = 0.3$. In all cases the noise strength is $D = 0.25$ and the coupling parameter is $\theta = 0.5$.

of the minimum, the shape of the distribution is practically independent of the system size. Indeed, the shapes are almost identical for $N = 100$ (circles) and $N = 1000$ (triangles). For each value of N, the corresponding stationary distribution is reached independently of the initial preparation of the system. In contrast, within the NLFPE, there are two single-particle distribution functions with just a single peak (solid lines). The system reaches one or the other depending upon whether the initial condition is centered initially around $x > 0$ or $x < 0$. The NLFPE has also in this region an unstable third solution describing a distribution centered around $x = 0$. Any slight initial deviation from it forces the system to go quickly to one of the two stable ones.

It should be pointed out that for any finite system the long-time stationary solution of the linear Fokker-Planck equation is given by Eq. (5). Then, due to the symmetry of the potential U and the fact that all the particles are identical, it follows that the single-particle distribution is symmetrical around the origin $x = 0$ and consequently the stationary average equilibrium value reached in the long-time limit has to be zero. This is consistent with the simulations of the Langevin equations but at variance with the results obtained with the NLFPE. The discrepancies between the simulation results and those obtained within the NLFPE are also evident in Fig. 6. In that figure we plot the time evolution of $M_1(t)$ as obtained from the numerical simulations of the Langevin equations for $N = 10$ and two different initial conditions (red solid lines) as well as the evolutions given by the NLFPE for two different initial conditions (black dashed lines). Note that the long-time limit of the first moment $M_1(t)$ as given by the NLFPE depends on the initial condition, while the simulation results indicate that for a given set of system parameters, the long-time limit is independent of the initial preparation.

For parameter values such that the NLFPE has just a single stable distribution, such as those depicted in Figs. 2 and 4, $M_1(t)$ relaxes quite quickly to its zero stationary value regardless of the system size or the initial condition. In contrast, for those parameter values such that the NLFPE has two stable distributions, the $M_1(t)$ relaxation time toward its zero stationary value is strongly dependent on N, as illustrated in Fig. 7, where we depict the time evolution of the first moment $M_1(t)$ obtained from numerical simulations of the Langevin equations for $D = 0.25$, $\theta = 0.5$, and $N = 100$ (lower curve), $N = 1000$ (middle curve), and $N = 10\,000$ (higher curve). The relatively large band of $M_1(t)$ values for larger sizes is due to the small number of noise realizations used in the simulations of those large systems. It seems interesting to compare the time evolution of the noise average $M_1(t)$ with that of a single trajectory $x_1(t)$. In Fig. 8 we depict the time evolution of the noise average of a single variable obtained from the numerical simulations of the Langevin equations by averaging over 500 noise realizations [$M_1(t)$, lower triangles] and the time evolution with a single noise realization [$x_1(t)$, solid line] for $N = 1500$, $D = 0.25$, and $\theta = 0.5$. The statistical effect of noise averaging is clear. In a single trajectory the variable explores the different potential minima with random transitions among them. The randomness of those jumps makes the noise average-time behavior very different with no jumps between the minima but with a monotonic decay towards its stationary zero value.

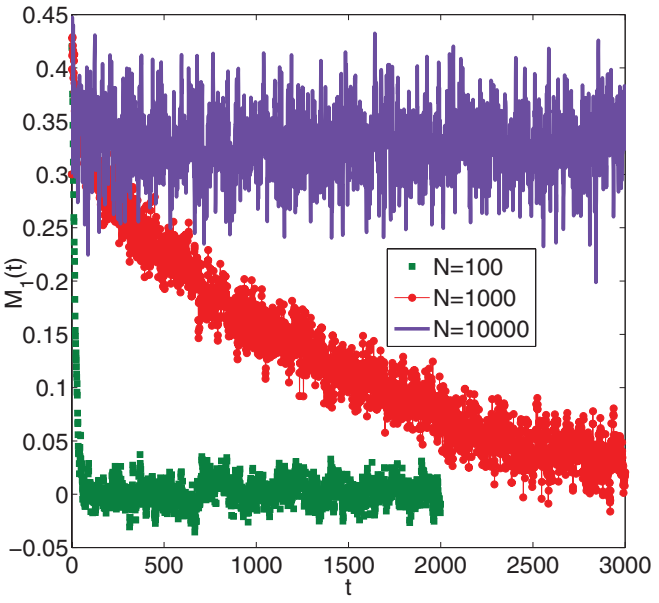

FIG. 7. (Color online) Time evolution of $M_1(t)$ obtained from the numerical simulations of the Langevin equations for the $N = 100$ (green bottom curve), $N = 1000$ (red middle curve), and $N = 10\,000$ (purple top curve). In all cases the noise strength is $D = 0.25$ and the coupling parameter is $\theta = 0.5$.

An estimation of the characteristic relaxation time of $M_1(t)$ from a given initial condition can be obtained by fitting the overall time evolution to an exponential. From the inverse of the exponent we have estimated the $M_1(t)$ relaxation time $t_{\rm rxn}$. In Fig. 9 we depict the natural logarithm of $t_{\rm rxn}$ for $D = 0.25$

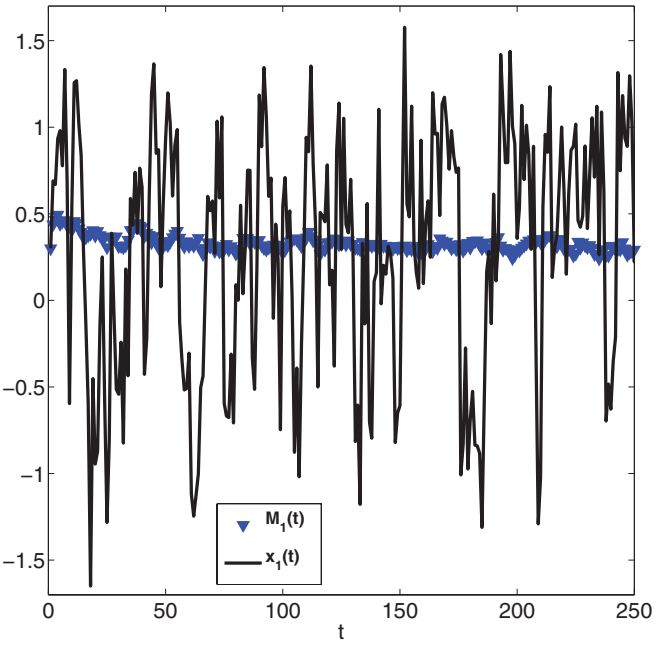

FIG. 8. (Color online) Time evolution of the noise average evolution of a single variable obtained from the numerical simulations of the Langevin equations by averaging over 500 noise realizations [$M_1(t)$, blue triangles] and the time evolution with a single noise realization [$x_1(t)$, black solid line] for $N = 1500$, $D = 0.25$, and $\theta = 0.5$.

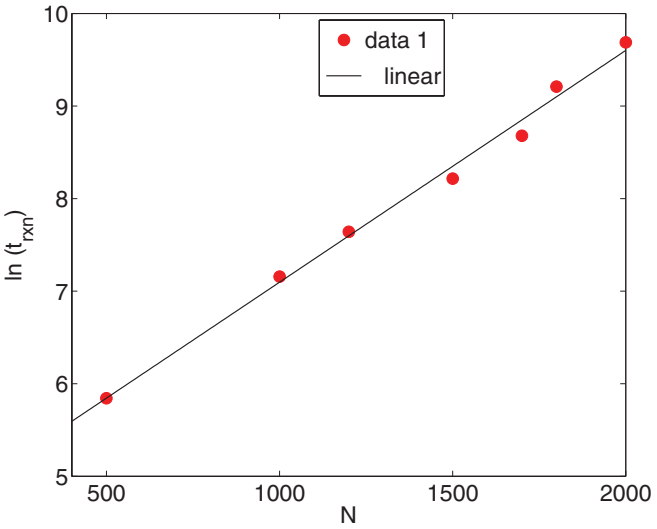

FIG. 9. (Color online) Natural logarithm of the relaxation time ($t_{\rm rxn}$) of $M_1(t)$ vs the system size. In all cases the noise strength is $D = 0.25$ and the coupling parameter is $\theta = 0.5$. The red dots correspond to the data, while the black line is the fit indicated in the main text.

and $\theta = 0.5$ for several values of N. The results for $N \geqslant 500$ are well fitted by the linear relation $\ln t_{\rm rxn} = 0.0025N + 4.6$.

The short-time behavior of $M_1(t)$ is depicted in Fig. 10 for several values of N. By short time we mean here time intervals long enough for small systems to reach their equilibrium state, but short compared to the total relaxation time of large systems. For sufficiently large systems, if we gather information during these short times to construct a histogram that mimics f_1, we find a distribution with a shape reminiscent of one of the two

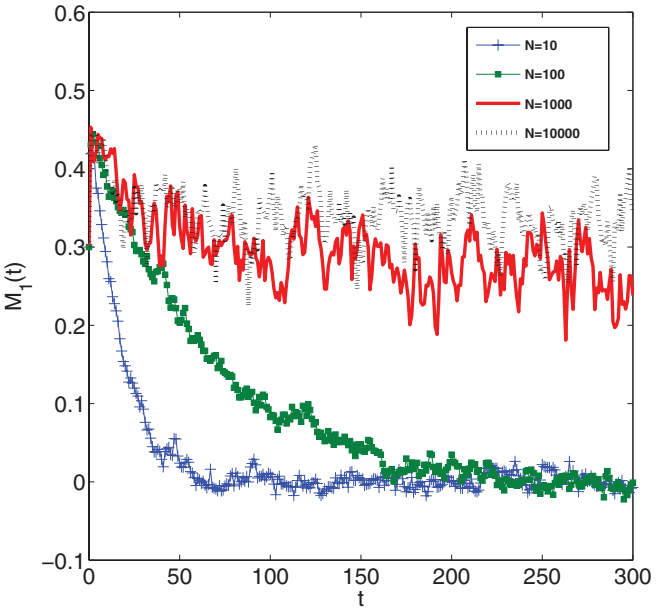

FIG. 10. (Color online) Short-time evolution of $M_1(t)$ obtained from the numerical simulations of the Langevin equations for $N = 10$ (blue plus signs), $N = 100$ (green dots), $N = 1000$ (red solid line), and $N = 10\,000$ (black dashed line). In all cases the noise strength is $D = 0.25$ and the coupling parameter is $\theta = 0.5$.

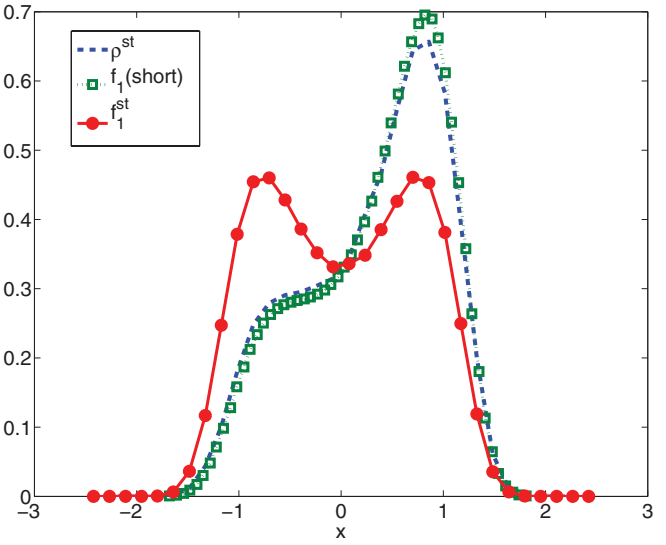

FIG. 11. (Color online) Single-particle distribution obtained from short numerical simulations of the Langevin equations (green squares) and long-time simulations for $N = 1000$ (red dots) as well as from the stationary solution of the NLFPE (blue dashed line). In all cases the noise strength is $D = 0.25$ and the coupling parameter is $\theta = 0.5$.

stable NLFPE distributions as depicted in Fig. 11 for a system with $N = 1000$, $D = 0.25$, and $\theta = 0.5$. In contrast, if we wait long enough for the system to reach a stationary state, then $f_1^{\rm st}$ differs largely from ρ as seen also in Fig. 11. For much larger systems, for instance, $N = 10\,000$, the relaxation is so slow and the duration of the transient regime is so large that the system stays in a sort of metastable state, with the single-particle distribution being very well approximated by $\rho^{\rm st}$ for very large observation times, as illustrated in Fig. 12 for a system with $N = 10\,000$ elements. The time it takes such a large system to reach its stationary distribution $f_1^{\rm st} \neq \rho^{\rm st}$ is

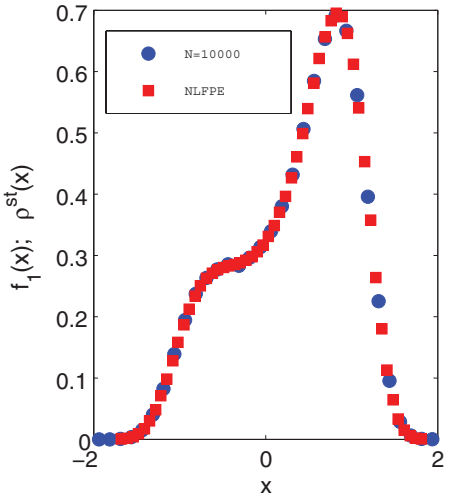

FIG. 12. (Color online) The short-time single-particle distribution function obtained from the simulations of Eq. (1) (blue circles) for a large system ($N = 10\,000$) matches the long-time stationary solution of Eq. (9) (red squares) very well. The other parameters are $D = 0.25$ and $\theta = 0.5$.

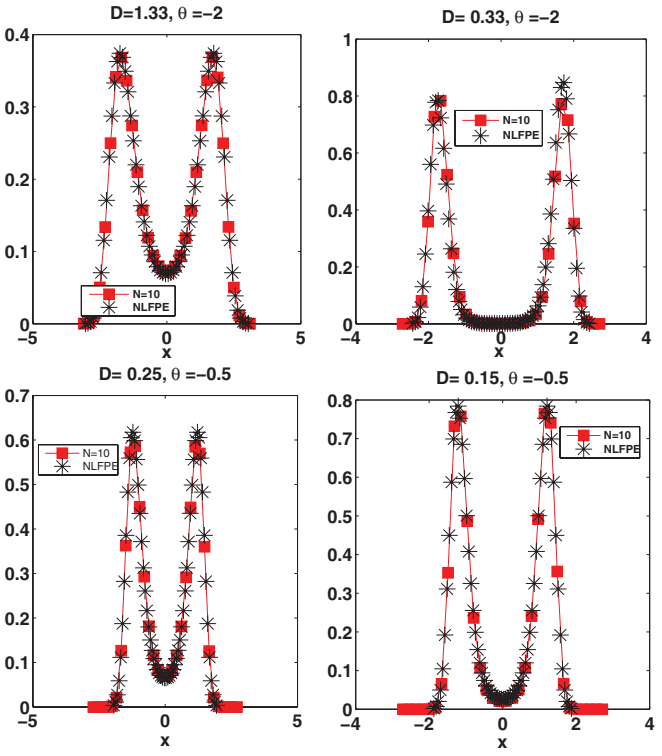

FIG. 13. (Color online) Single-particle stationary distribution function obtained from the simulations of Eq. (1) (red squares) and the stationary solution of Eq. (9) (black stars) for several values of the system parameters.

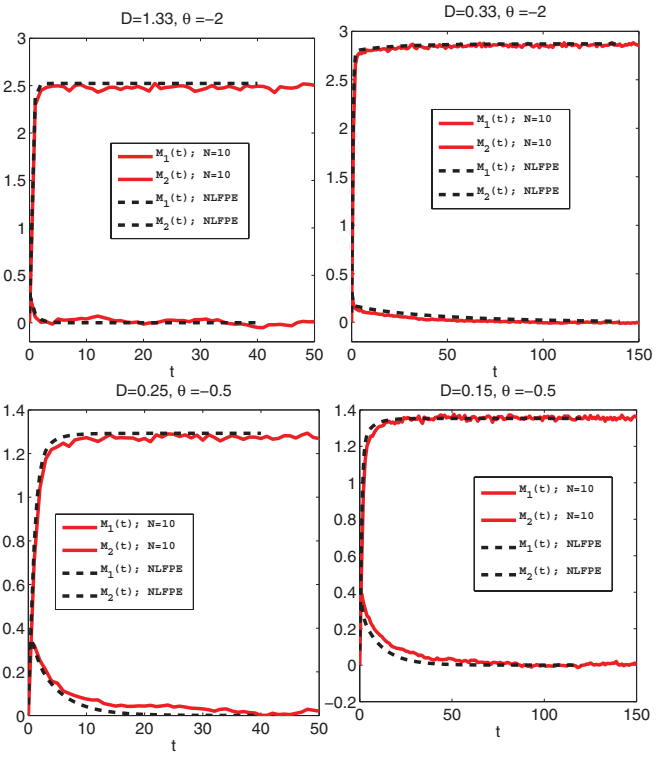

FIG. 14. (Color online) The bottom solid red line depicts the time evolution of $M_1(t)$ while the top solid red line depicts the evolution of $M_2(t)$ obtained from the simulations of Eq. (1). The black dashed lines depict the corresponding evolutions obtained from the solution of Eq. (7).

extremely long compared with the already very long transient time.

B. The case of negative θ

We now turn our attention to the model with a negative mean-field coupling parameter $\theta < 0$. An extensive numerical treatment of Eqs. (9) and (10) leads to the conclusion that for $\theta < 0$, $X_0 = 0$ is the only stationary solution and consequently there is just one stable stationary solution for the NLFPE description. In Fig. 13 we plot the stationary distributions obtained within the NLFPE and by Langevin simulations for a system of just $N = 10$ elements and for a variety of system parameters. In Fig. 14 the results of the time evolution of the first two moments obtained from the Langevin simulations are compared with those obtained by solving the NLFPE (9). As one can see, the NLFPE provides an excellent description of the relaxation dynamics as well as the stationary distribution for all the parameter values, even for a system of rather modest size ($N = 10$).

IV. CONCLUSION

In this work we have analyzed the reliability of the SCDMF approximation to describe the statistical behavior of a single particle immersed in a finite array of interacting identical particles. The lack of analytical solutions has lead us to investigate the problem by means of numerical schemes. The NLFPE has been numerically integrated and the results have been compared with those provided by numerical simulations of the Langevin equations for the array.

We have found that the sign of the parameter characterizing the strength of the interaction θ is very relevant. For positive values of θ, the SCDMF approximation provides a good description of the relaxation dynamics and the stationary distribution as long as we deal with system parameters (noise and interaction strengths) such that the NLFPE derived within the SCDMF has only one stationary solution.

In contrast, for system parameter values such that the NLFPE has two independent stable stationary solutions, the results of this asymptotic approximation are qualitatively and quantitatively different from those obtained from the Langevin (or Fokker-Planck) description of small finite systems. Nonetheless, the NLFPE leads to stable distributions that are remarkably similar to those obtained during the Langevin simulations of large-size systems using short trajectories.

Thus, for $\theta > 0$ the SCDMF does not seem to provide a consistent approximation to describe the single-particle behavior of an N-particle system for all regions of parameter space. The approximation leads to a close equation for the single-particle distribution but at the expense of introducing spurious qualitative features absent in the dynamics of finite systems.

The case is different for $\theta < 0$. In this case the NLFPE has only a single long-time stationary solution for all parameter values, centered around $x = 0$, to which the system relaxes regardless of its initial preparation. The description of the

dynamics for finite systems provided by the numerical simulations is basically identical to that obtained within the NLFPE, even for very small sizes.

ACKNOWLEDGMENTS

We acknowledge the support of the Ministerio de Ciencia e Innovación of Spain (Grant No. FIS2008-04120)

[1] K. Kometani and H. Shimizu, J. Stat. Phys. **13**, 473 (1975).
[2] R. C. Desai and R. Zwanzig, J. Stat. Phys. **19**, 1 (1978).
[3] R. A. Dawson, J. Stat. Phys. **31**, 29 (1983).
[4] M. Shiino, Phys. Rev. A **36**, 2393 (1987).
[5] R. Toral and C. J. Tessone, Commun. Comput. Phys. **2**, 177 (2007).
[6] A. R. Bulsara and G. Schmera, Phys. Rev. E **47**, 3734 (1993).
[7] J. M. Casado, J. Gómez-Ordóñez, and M. Morillo, Phys. Rev. E **73**, 011109 (2006).
[8] J. M. Casado, J. Gómez-Ordóñez, and M. Morillo, Europhys. Lett. **79**, 50002 (2007).
[9] A. Pikovsky, A. Zaikin, and M. A. de la Casa, Phys. Rev. Lett. **88**, 050601 (2002).
[10] M. Morillo, J. Gómez-Ordóñez, and J. M. Casado, Eur. Phys. J. B **74**, 211 (2010).
[11] T. Vaz Martins, V. N. Livina, A. P. Majtey, and R. Toral, Phys. Rev. E **81**, 041103 (2010).
[12] J. Gómez-Ordóñez, J. M. Casado, M. Morillo, C. Honisch, and R. Friedrich, Europhys. Lett. **88**, 40006 (2009).
[13] A. N. Drozdov and M. Morillo, Phys. Rev. E **54**, 931 (1996).
[14] R. Balescu, *Equilibrium and Nonequilibrium Statistical Mechanics* (Wiley, New York, 1975).
[15] J. Casado-Pascual, C. Denk, J. Gómez-Ordóoñez, M. Morillo, and P. Hänggi, Phys. Rev. E **67**, 036109 (2003).